RJC

RASĀYAN *J. Chem.*
Vol. 18 | No. 3 |1274-1281| July-September | 2025
ISSN: 0974-1496 | e-ISSN: 0976-0083 | CODEN: RJCABP
http://www.rasayanjournal.com
http://www.rasayanjournal.co.in

INFLUENCE OF THE PUSH-PULL CHROMOPHORIC EFFECT OF AMINO GROUPS ON THE DIPOLE MOMENTS OF 7-SUBSTITUTED-2-(4-HALOPHENYL)IMIDAZO [1,2-A]PYRIDINE -BASED STYRYL DYES VIA SOLVATOCHROMIC ANALYSIS

D. B. Yedage[1], K.A. Mestry[2], D.V. Patil[2] and S.D. Jadhav[1,✉]
[1]Department of Chemistry, Willingdon College, Sangli(MH)- 416415, India
[2]Department of Chemistry, Kirti M. Doongursee College, Dadar (W), Mumbai-400028, India
✉Corresponding author: sdjchem@gmail.com

ABSTRACT

This research explores the dipole moments in both the excited and ground states for a series of 7-substituted-2-(4-chlorophenyl)imidazo[1,2-a]pyridine-based styryl dyes, incorporating different electron-donating groups. Amino-substituted imidazopyridines with piperidinylamino, diethylamino, and dimethylamino groups were studied, along with one unsubstituted reference. Their solvatochromic performance was examined in solvents of various polarities (toluene, tetrahydrofuran, dichloromethane, acetonitrile, and dimethyl sulfoxide) using UV-Visible absorption and fluorescence spectroscopy. Multiple theoretical models were used to check excited-state dipole moments, accompanied by DFT and TD-DFT calculations, and studied alongside the unsubstituted compound. The amino-substituted derivatives exhibited significant bathochromic shifts in emission with increasing solvent polarity, with Stokes shifts reaching 6401 cm¹ for the piperidinylamino compound in acetonitrile. The derivative with the diethylamino substituent demonstrated the highest dipole moments in both ground (8.16 D) and excited states (up to 14.80 D), indicating enhanced intramolecular charge transfer character. The strong correlation between spectroscopic data and solvent polarity functions for amino-substituted derivatives, particularly the dimethylamino compound (R^2 = 0.9157-0.9740), validates their potential as solvatochromic probes. These findings provide crucial insights for designing advanced optoelectronic materials based on the 7-Substituted-2-(4-halophenyl)imidazo[1,2-a]pyridine Styryl scaffold with tailored photophysical properties.

Keywords: Solvatochromism, Dipole Moment, Intramolecular Charge Transfer, DFT, NLO, Styryl Dyes.
RASĀYAN *J. Chem.*, Vol. 18, No.3, 2025

INTRODUCTION

Investigating dipole moments in both ground and excited states offers valuable insights into the electronic characteristics and molecular interactions of organic compounds. Solvatochromism, which describes the spectral shift of a molecule due to changes in solvent polarity, plays a crucial role in understanding electronic transitions and charge transfer mechanisms.[1] The presence of donor-acceptor (D-π-A) systems in organic molecules, especially those exhibiting a push-pull chromophoric effect, significantly influences their nonlinear optical (NLO) properties, making them essential in advanced optical and electronic applications.[2] Styryl dyes, especially those based on the imidazo[1,2-a]pyridine nucleus, represent a notable set of compounds due to their strong electronic conjugation & extreme fluorescence quantum yield.[3] These dyes are widely applied in optoelectronic devices, sensors, biological imaging, and organic light-emitting diodes (OLEDs). The incorporation of an electron-donating amino group strengthens the push-pull nature of these dyes, resulting in significant twisted intramolecular charge transfer (TICT) and intramolecular charge transfer (ICT) effects. These effects result in substantial differences amongst the dipole moments of both states, impacting their solvatochromic behavior and overall photophysical properties.[4] The existence of an amino group (-NH2) in styryl dyes established on the imidazo[1,2-a]pyridine nucleus significantly affects the electronic structure and dipole moments of these compounds. The amino group acts as a strong electron donor, enhancing charge delocalization within the π-conjugated system.[5] This donor effect increases the polarity of the molecule in both states, leading to higher dipole moments compared to dyes without an amino substituent.

Rasayan J. Chem., 18(3), 1274-1281(2025)
http://doi.org/10.31788/RJC.2025.1839300

This work is licensed under a CC BY 4.0 license.

In the ground state, the amino group contributes to an improvement in electron density around the donor site, reinforcing the dipole moment. However, upon excitation, a substantial redistribution of charge occurs, leading to a greater increase in dipole moment due to the strong ICT effect. This behavior is particularly evident in polar solvents, where solvent stabilization further enhances dipole moment differences between the ground and excited states.[6] Experimental and computational studies have shown that the amino-substituted styryl dyes exhibit red-shifted absorption and emission spectra compared to their non-substituted counterparts. This red shift occurs due to enhanced intramolecular charge transfer (ICT), which becomes stable in the excited state relative to the ground state. The degree of this stabilization depends on the nature of the solvent, with highly polar solvents amplifying the charge separation effect. As a result, amino-functionalized styryl dyes show pronounced solvatochromic behavior, making them valuable candidates for applications in fluorescence sensing, dye lasers, and other optoelectronic devices.[7] Given the importance of dipole moment variations in the design of advanced optoelectronic materials, this study aims to investigate both dipole moments of styryl dyes using solvatochromic methods.[8] The effects of different solvents on these dipole moments are explored, providing a comprehensive understanding of solvent-induced spectral shifts. A comprehensive approach utilizing multiple theoretical models was employed to analyze the correlation between solvent properties and spectral shifts observed in these compounds. Using the unsubstituted imidazo[1,2-a]pyridine-based styryl dye as a reference point, this work correlating experimental findings with computational studies, this work seeks to establish a systematic approach for predicting and optimizing the optical characteristics of imidazo[1,2-a] pyridine-based styryl dyes for future technological applications.[9]

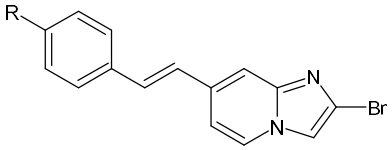

R= H, NMe_2,NEt_2, $N(CH_2)_5$

Fig.-1: General Structures 7-Substituted-imidazo[1,2-a]pyridine

EXPERIMENTAL

The dipole moments of styryl dyes in both states were determined using multiple solvatochromic methods, which rely on the relationship between polarity and spectral shifts of absorption & emission maxima. These calculations were carried out based on well-established quantum mechanical models, incorporating second-order perturbation theory and solvent polarity functions.

Bilot-Kawski Method I

The Bilot-Kawski method, derived from second-order perturbation theory, correlates the Stokes shift (difference between absorption & emission maxima) with solvent polarity functions as $f_1(\varepsilon, n)$ and $f_2(\varepsilon, n)$ Where the dielectric constant (ε) and refractive index (n) are the solvents.[10] The equations governing this method are:

$$\bar{\vartheta}_{abs} - \bar{\vartheta}_{emn} = \left[\frac{2(\mu_e - \mu_g)^2}{hca^3}\right] f_1(\varepsilon, n) + \text{Constant} \quad (1)$$

$$\left(\frac{\bar{\vartheta}_{abs} + \bar{\vartheta}_{emn}}{2}\right) = \left[\frac{-2(\mu_e{}^2 - \mu_g{}^2)}{hca^3}\right] f_2(\varepsilon, n) + \text{Constant} \quad (2)$$

Here, $\bar{\vartheta}_{abs}$ and and $\bar{\vartheta}_{emn}$ Represents the absorption & emission maxima wavenumbers, respectively. Where μ_e = ground μ_g= excited dipole moment, Planck's constant (h), velocity of light (c), and Onsager's cavity radius (a). The solvent polarity functions $f_1(\varepsilon, n)$ and $f_2(\varepsilon, n)$ are defined as

$$f_1(\varepsilon, n) = \left[\frac{2n^2+1}{n^2+2}\right] \cdot \left[\frac{\varepsilon-1}{\varepsilon+2} - \frac{n^2-1}{n^2+2}\right] \quad (3)$$

$$f_2(\varepsilon, n) = \frac{1}{2} f_1(\varepsilon, n) + \frac{3}{2}\left[\frac{n^4-1}{(n^2+2)^2}\right] \quad (4)$$

By plotting $f_1(\varepsilon, n)$ against the Stokes shift and $f_2(\varepsilon, n)$ against the arithmetic mean of absorption & emission wavenumbers, slopes m_1 and m_2 Are obtained. These slopes are employed to evaluate both state dipole moments:

$$\mu_g = \frac{(m_2 - m_1)}{2}\left[\frac{hca^3}{2m_1}\right]^{1/2} \quad \text{and} \quad \mu_e = \frac{(m_2 + m_1)}{2}\left[\frac{hca^3}{2m_1}\right]^{1/2} \tag{5}$$

Additionally, the angle φ among the two state dipole moments is estimated by the equation

$$\cos\varphi = \frac{1}{2\mu_g\mu_e}\left[\left({\mu_g}^2 + {\mu_e}^2\right) - \frac{m_1}{m_2}\left({\mu_e}^2 - {\mu_g}^2\right)\right] \tag{6}$$

Lippert-Mataga Method II: The Lippert-Mataga Equation relates the Stokes shift to the function $f_{LM}(\varepsilon, n)$.[11]

$$\bar{\vartheta}_{abs} - \bar{\vartheta}_{emn} = \frac{2(\mu_e - \mu_g)^2}{hca^3} f_{LM}(\varepsilon, n) + Constant \tag{7}$$

Here, $$f_{LM}(\varepsilon, n) = \frac{\varepsilon - 1}{2\varepsilon + 1} - \frac{n^2 - 1}{2n^2 + 1}$$

The slope is m_{LM} is applied to assess the excited-state dipole moment

$$\mu_e = \sqrt{\frac{m_{LM} hca^3}{2}} + \mu_g$$

Bakhshiev Method III: The Bakhshiev method employs a similar approach, with the solvent polarity function $f_{BK}(\varepsilon, n)$ [12].

$$\bar{\vartheta}_{abs} - \bar{\vartheta}_{emn} = \frac{2(\mu_e - \mu_g)^2}{hca^3} f_{BK}(\varepsilon, n) + Constant \tag{8}$$

Here, $$f_{BK}(\varepsilon, n) = \left[\frac{2n^2 + 1}{n^2 + 2}\right] . \left[\frac{\varepsilon - 1}{\varepsilon + 2} - \frac{n^2 - 1}{n^2 + 2}\right]$$

The slope is m_{BK}It helps to decide the excited state dipole moment...

$$\mu_e = \sqrt{\frac{m_{BK} hca^3}{2}} + \mu_g$$

Kawaski-Chamma-Viallet Method IV: Kawaski-Chamma-Viallet Method uses a method of solvent function $f_{KCV}(\varepsilon, n)$[13]

$$\frac{\bar{\vartheta}_{abs} - \bar{\vartheta}_{emn}}{2} = \frac{-2\left({\mu_e}^2 - {\mu_g}^2\right)}{hca^3} f_{KCV}(\varepsilon, n) + Constant \tag{9}$$

Here, $$f_{KCV}(\varepsilon, n) = \left[\frac{2n^2 + 1}{2(n^2 + 2)}\right]\left(\frac{\varepsilon - 1}{\varepsilon + 2} - \frac{n^2 - 1}{n^2 + 2}\right) + \frac{3}{2}\left[\frac{n^4 - 1}{(n^2 + 2)^2}\right]$$

The slope $m_{KCV}It$ It is applied to compute the excited-state dipole moment.

$$\mu_e = \sqrt{\frac{(-m_{KCV}) hca^3}{2} + {\mu_g}^2}$$

Reichardt solvent polarity function Method V: The Reichardt method employs the microscopic solvent polarity parameter $\mathrm{E_T^N}$, which accounts for specific solute-solvent interactions:[14]

$$\bar{\vartheta}_{abs} - \bar{\vartheta}_{emn} = (m_{\mathrm{E_T^N}})\mathrm{E_T^N} + Constant \tag{10}$$

The slope $m_{\mathrm{E_T^N}}$ is used to calculate the differentiation between the excited & ground state dipole moments

$$\mu_e = \sqrt{\frac{m_{\mathrm{E_T^N}} 81}{11307.6\left(\frac{6.2}{a_0}\right)^3}} + \mu_g \tag{11}$$

Where, $m_{\mathrm{E_T^N}}$ is slope.

Computational Optimization Method V

The molecular structures were computationally optimized at ground state using the B3LYP functional shared alongside the 6-31G(d) basis set, providing an effective compromise between computational resources and result precision.[15] An Onsager cavity radius was calculated using Gaussian's volumetric analysis tools, which was subsequently applied in the experimental dipole moment determinations. To examine solvent-influenced electronic transitions, time-dependent density functional theory calculations were conducted utilizing the SCRF methodology with the Polarizable Continuum Model implemented across the five experimental solvents.[16] This theoretical framework successfully captured the solvent-dependent spectroscopic phenomena and provided computational confirmation of the experimentally determined enhanced intramolecular charge transfer character observed in the amino-functionalized derivatives.[17]

RESULTS AND DISCUSSION

The studied dyes are as follows: Unsubstituted S1, substituted S2, 4-diethylamino substituted S3, and 4-dimethyl substituted S4. The values of the solvent polarity functions $f_2(\varepsilon, n)$, $f_{LM}(\varepsilon, n)$, $f_{BK}(\varepsilon, n)$, $f_{KCV}(\varepsilon, n)$ And microscopic molecular sol. function E_T^N For the different solvents & solvent combinations examined in this study and presented in Table-1. The solvent polarity function $f_2(\varepsilon, n)$, $f_{LM}(\varepsilon, n)$, $f_{BK}(\varepsilon, n)$, $f_{KCV}(\varepsilon, n)$ & E_T^N They were analyzed for various solvents and their mixtures, as outlined in Table-1 of this study. Refractive index & relative permittivity values of mixtures were used to determine the primary solvent polarity, which were computed following Equations 3–4 and 8–11.

Table-1: Examined Solvents Polarity Chart

Solvents[a]	Toluene	Tetrahydrofuran	Dichloromethane	Acetonitrile	Dimethyl sulfoxide
ϵ^b	2.38	7.58	8.93	37.5	46.7
n^c	1.4969	1.4072	1.4242	1.3441	1.4793
$f_1(\varepsilon, n)$	0.1147	0.6097	0.6555	0.908	0.9205
$f_2(\varepsilon, n)$	0.7854	1.1629	1.2312	1.3767	1.5685
$f_{LM}(\varepsilon, n)^d$	0.0132	0.2096	0.2171	0.3054	0.2631
$f_{BK}(\varepsilon, n)^e$	0.0291	0.5491	0.5903	0.8631	0.84
$f_{KCV}(\varepsilon, n)^f$	0.3499	0.5511	0.583	0.6659	0.7442

Abbreviations: [b]Dielectric constant of solvent, [c]Refractive Index of solvent, [d]Lippart-Mataga polarity function of solvent, [e]Bakhshiev function, [f]KCV function, [g]Reichardt function

The solvent polarity functions shown in Table-1 provide a foundation for understanding the solvent-solute interactions in this study. These parameters represent different approaches to quantifying solvent polarity, with each function emphasizing specific aspects of solvent-solute interactions. The values for solvents show a progressive increase in polarity, with toluene being the least polar (ε = 2.38) and DMSO being the most polar (ε = 46.7) among the studied solvents. The absorption (λa), emission (λb) wavelength, Stokes shift (Δϒ), the mathematical mean of the Stokes shift value [x= $\left(\frac{\bar{\vartheta}_{abs} + \bar{\vartheta}_{emn}}{2}\right)$] in ($cm^{-1}$) and summation absorption-emission in cm-1 (y= $\bar{\vartheta}_{abs} + \bar{\vartheta}_{emn}$) are represented in Table-2. The absorption and emission maxima data presented in Table-2 reveal significant solvatochromic effects across all four dyes. Compound S1, which lacks an amino substituent, shows the least pronounced solvatochromic shift with Stokes values ranging from 994 cm^{-1} in toluene to 2700 cm^{-1} in acetonitrile. In contrast, the amino-substituted derivatives (S2-S4) exhibit considerably sizable Stokes shifts, with values reaching up to 6401 cm^{-1} for S2 in acetonitrile.

Table-2: Solvatochromic Properties in Various Solvents

Solvents	S1						S2				
	λa	λf	Δϒ	X	y		λa	λf	ΔϒΥ	x	y
Toluene	381	396	994	25750	51499		376	459	4809	24191	48382
THF	379	416	2347	25212	50424		374	467	5325	24076	48151
DCM	377	395	1209	25921	51842		374	479	5861	23807	47615
ACN	374	416	2700	25388	50776		373	490	6401	23609	47218
DMSO	381	423	2606	24944	49887		382	497	6057	23149	46299
Solvents	S3						S4				

	λa	λf	ΔϒΔ	X	y		λa	λf	ΔϒΔ	x	y
Toluene	388	434	2732	24407	48815		384	434	3000	24542	49083
THF	384	417	2061	25011	50022		382	461	4486	23935	47870
DCM	386	475	4854	23480	46959		379	471	5154	23808	47617
ACN	383	488	5618	23301	46601		384	486	5466	23309	46618
DMSO	392	495	5308	22856	45712		384	492	5716	23183	46367

A closer examination of the data reveals several important trends. The absorption maxima (λ_a) for all compounds show minimal solvatochromic shifts across different solvents, with variations of only 3-9 nm. This suggests that the ground state is less affected by polarity with respect to the excited state. The emission maxima (λ_f) demonstrate substantial bathochromic shifts with increasing solvent polarity, particularly for compounds S2-S4. For instance, S2 shows a 38 nm red shift in emission when moving from toluene (459 nm) to DMSO (497 nm). This indicates significant preservation of the excited state in polar solvents. The Stokes shift values (ΔϒΔ) consistently increase with solvent polarity for all compounds, with the amino-substituted derivatives (S2-S4) showing significantly larger shifts compared to S1. This confirms that the introduction of electron-donating amino groups enhances the ICT character of these dyes. The arithmetic mean of absorption and emission wavenumbers (x) shows a declining trend with increasing solvent polarity, particularly for the amino-substituted derivatives. This decrease indicates that the excited state experiences greater stabilization than destabilization of the ground state in polar media. For the estimation of dipole moments, graphs are plotted for various functions $(\bar{\vartheta}_{abs} - \bar{\vartheta}_{emn})$ against $f_1(\varepsilon, n)$, $(\bar{\vartheta}_{abs} + \bar{\vartheta}_{emn})$ against $f_2(\varepsilon, n)$ For Bilot Kawaski, $(\bar{\vartheta}_{abs} - \bar{\vartheta}_{emn})$ against $f_{LM}(\varepsilon, n)$ for Lippert-Mataga, $(\bar{\vartheta}_{abs} - \bar{\vartheta}_{emn})$ against $f_{BK}(\varepsilon, n)$ for Bakhshiev, $\left(\frac{\bar{\vartheta}_{abs} + \bar{\vartheta}_{emn}}{2}\right)$ against $f_{KCV}(\varepsilon, n)$ for K.C.V. and $(\bar{\vartheta}_{abs} - \bar{\vartheta}_{emn})$ polarity function. The corresponding values are provided in Table-3.

Table-3: Regression Coefficients and Slope of Various Colorants Across Functions

	S1		S2		S3		S4	
	Slope	R.C.	Slope	R.C.	Slope	R.C.	Slope	R.C.
$f_1(\varepsilon, n)$	2019	0.6677	1801	0.8780	3596	0.5337	3265	0.9618
$f_2(\varepsilon, n)$	-1759	0.4162	-2611	0.8437	-4402	0.5320	-3671	0.9656
$f_{LM}(\varepsilon, n)$	5758	0.6392	5206	0.8638	9634	0.4509	9286	0.9157
$f_{BK}(\varepsilon, n)$	1968	0.6711	1759	0.8854	3470	0.5254	3164	0.9550
$f_{KCV}(\varepsilon, n)$	-1693	0.4016	-2513	0.8137	-4240	0.5141	-3613	0.9740

R.C.= Regression Coefficient

Data presents the slopes and regression coefficients obtained from various theoretical models applied to determine the dipole moments. The correlation between spectroscopic data and solvent polarity functions reveals important insights. For compound S1, which is without substitution of the amino group, the correlation coefficients are relatively low (0.4016-0.6711) across all functions, suggesting a weaker dependence on solvent polarity. This is consistent with the ordinary solvatochromic shifts observed for this compound. Polarity graphs are represented for the first two functions in Fig.-2.

Compounds S2-S4, featuring amino substituents, show improved correlation coefficients, with S4 (containing the dimethylamino group) demonstrating the strongest correlations (0.9157-0.9740). This indicates that the presence of electron-donating groups enhances the sensitivity of these dyes to solvent polarity. The negative slopes observed for $f_2(\varepsilon, n)$ and $f_{KCV}(\varepsilon, n)$ functions across all compounds indicate a decrease in the sum of absorption and emission energies with increasing solvent polarity, further confirming the notable steadying of the excited state compared to the ground state. The magnitude of slopes increases significantly from S1 to S3, with S3 showing the largest values. This suggests that the diethylamino substituent in S3 provides the strongest electron-donating effect among the studied compounds. Both state dipole moments calculated employing various methods are mentioned in Table-4, revealing several significant trends. The experimentally estimated ground state dipole moments using the Bilot-Kawaski (B-K) method are notably lower (0.40–1.41 D) than those calculated theoretically via density functional theory (DFT) (5.04–8.16 D), likely due to experimental limitations or theoretical assumptions regarding molecular geometry and electronic distribution.

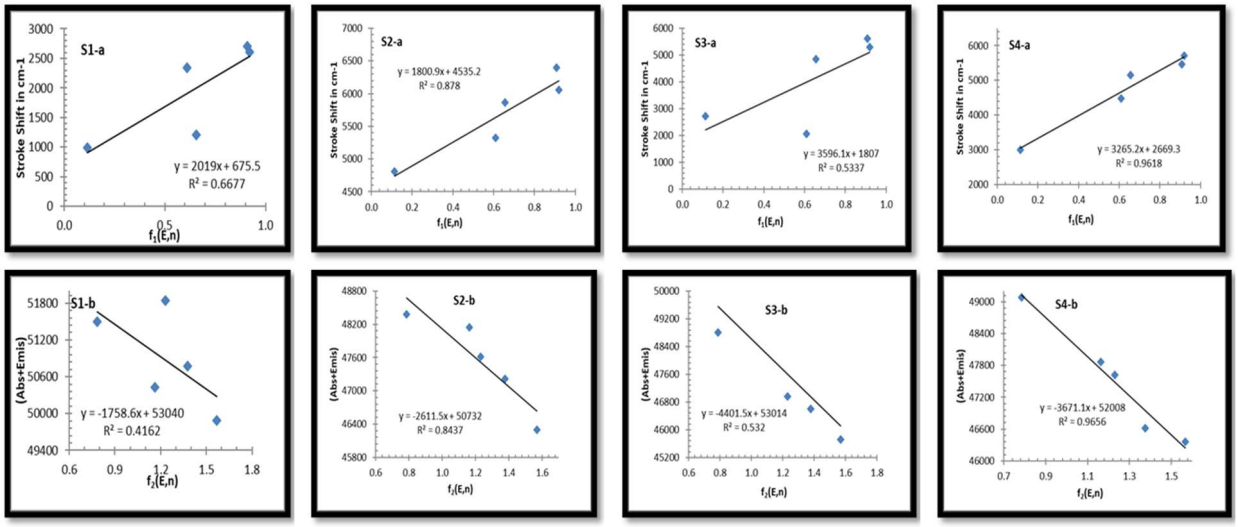

Fig.-2: Linear Plots of Dyes S1 to S4 of different Functions for Bilot–Kawski

Table-4: Dipole Moments of Various Styryls and Measured in Debye, D

Dyes	GS DM[b]		Excited State dipole moment					
	B-K[c]	DFT[d]	TD-DFT[d]	B-K[c]	LM[e]	BK[f]	KCV[g]	Reich[h]
S1	0.40	5.04	6.26	5.73	10.75	6.45	5.63	6.28
S2	1.41	7.09	8.01	7.70	12.10	7.62	7.55	6.96
S3	0.95	8.16	9.84	9.41	14.80	9.26	9.24	9.86
S4	0.48	8.01	9.03	8.28	13.63	8.16	8.21	8.27

Abbreviations [a]Onsagar Cavity Radius in (A^0), [b]Dipole Moment (Ground State), [c]Bilot-Kawaski, [d]DFT & TDDFT, [e]Lippert Mataga, [f]Bakshiev, [KCV]KCV, and [h]Reichardt Models

Next level dipole moments are consistently higher than their ground state counterparts across all compounds and determination methods, confirming increased charge separation upon photoexcitation because of the intramolecular charge transfer (ICT) process characteristic of these push-pull chromophores. Among the various approaches for estimating excited state dipole moments, the Lippert-Mataga (LM) method yields the highest values (10.75–14.80 D), while the Kawski-Chamma-Viallet (KCV) method provides more conservative estimates (5.63–9.24 D), emphasizing the need for multiple theoretical frameworks to realise a broad insight of excited state properties. The amino-substituted derivatives (S2–S4) exhibit significantly higher dipole moments in both states compared to the unsubstituted compound (S1), with S3, featuring a diethylamino substituent, displaying the highest excited state dipole moment of 14.80 D according to the LM method. Furthermore, time-dependent DFT (TD-DFT) calculations produce excited state dipole moment values (6.26–9.84 D) that align well with experimentally obtained values from the Bakhshiev (BK) (6.45–9.26 D) and Reichardt (6.28–9.86 D) methods, reinforcing the reliability of both theoretical and experimental approaches.

Structure-Property Relationships

The observed variations in dipole moments and solvatochromic behavior among the four compounds can be directly linked to their structural differences. Compound S1, which lacks an amino substituent, exhibits the smallest alteration in dipole moment on excitation & the least pronounced solvatochromic shifts, indicating minimal charge transfer character. In contrast, the presence of amino substituents in compounds S2–S4 significantly enhances their dipole moments and solvatochromic responses. Among them, the diethylamino group in S3 proves to be the most effective electron donor, leading to the highest both state dipole moments. The piperidinylamino substituent in S2 results in intermediate dipole moment values, suggesting that the cyclic nature of piperidine may partially restrict the nitrogen lone pair's conjugative

participation. Interestingly, the dimethylamino group in S4 produces slightly lower dipole moments than the diethylamino group in S3, despite their structural similarity.

CONCLUSION

In the conclusion, this study provides a comprehensive analysis of the photophysical characteristics of styryl dyes, focusing on the influence of amino substituents on dipole moments and solvatochromic behavior. Dipole moments were determined through multiple theoretical models, ground state dipole moments ranging from 5.04 D (unsubstituted) to 8.16 D (diethylamino-substituted), with excited state values reaching up to 14.80 D using the Lippert-Mataga approach. The amino-substituted derivatives exhibited significant Stokes shifts (up to 6401 cm^{-1} in acetonitrile) compared to the unsubstituted reference (994-2700 cm^{-1}). These findings establish clear structure-property relationships, with the diethylamino compound showing the strongest dipole enhancement. The high correlation coefficients (R^2=0.9157-0.9740) for the dimethylamino derivative validate these compounds' potential as solvatochromic probes. The substantial dipole moment differences between ground and excited states ($\Delta\mu$ = 5.35-9.76 D) confirm enhanced intramolecular charge transfer upon amino substitution. This work provides crucial insights for designing advanced functional materials with the imidazo [1,2-a] pyridine scaffold.

ACKNOWLEDGMENTS

The authors acknowledge both colleges for supporting this research work.

CONFLICT OF INTERESTS

The authors declare that there is no conflict of interest.

AUTHOR CONTRIBUTIONS

The present work is related to *SDG-7: Affordable and Clean Energy*. All the authors contributed significantly to this manuscript, participated in reviewing/editing, and approved the final draft for publication. The research profile of the authors can be verified from their ORCID ids, given below:

S.D. Jadhav https://orcid.org/0000-0002-0678-039X
D.B. Yedage https://orcid.org/0000-0001-5660-5437
K.A. Mestry https://orcid.org/0009-0001-0514-5028
D. V. Patil https://orcid.org/0000-0003-0207-8891

Open Access: This article is distributed under the terms of the Creative Commons Attribution 4.0 International License (http://creativecommons.org/licenses/by/4.0/), which permits unrestricted use, distribution, and reproduction in any medium, provided you give appropriate credit to the original author(s) and the source, provide a link to the Creative Commons license, and indicate if changes were made.

REFERENCES

1. C. Reichardt, *Chemical Review,* **94(8)**, 2319(1994), https://doi.org/10.1021/cr00032a005
2. J. Gierschner, J. Cornil, and H. Egelhaaf, *Advanced Materials* **19(2)**, 173(2007), https://doi.org/https://doi.org/10.1002/adma.200600277
3. S. D. Jadhav, and N. Sekar, *Journal of Luminescence,* **190**, 289(2017), https://doi.org/https://doi.org/10.1016/j.jlumin.2017.05.066
4. P. Suppan, *Journal of Photochemistry and Photobiology A: Chemistry* **50(3)**, 293(1990), https://doi.org/https://doi.org/10.1016/1010-6030(90)87021-3
5. B. Aydıner, E. Yalçın, H. Ihmels, L. Arslan, L. Açık and Z. Seferoğlu, *Journal of Photochemistry and Photobiology A: Chemistry,* **310**, 113(2015), https://doi.org/https://doi.org/10.1016/j.jphotochem.2015.05.030
6. Z. R. Grabowski, K. Rotkiewicz, and W. Rettig, *Chemical Reviews,* **103(10)**, 3899(2003), https://doi.org/10.1021/cr9407451
7. C. Adamo and D. Jacquemin, *Chemical Society Reviews,* **42(3)**, 845(2013), https://doi.org/10.1039/C2CS35394F
8. N. Mataga, Y. Kaifu and M. Koizumi, *Bullettin of the Chemical Society of Japan,* **29(4)**, 465(1956), https://doi.org/10.1246/bcsj.29.465

9. J. Brédas, D. Beljonne,, V. Coropceanu and J. Cornil, *Chemical Reviews,* **104(11)**, 4971(2004), https://doi.org/10.1021/cr040084k
10. L. Bilot and A. Kawski, *Zeitschrift fur Naturforschung - Section A Journal of Physical Sciences,* **17(7)**, 621(1962), https://doi.org/10.1515/zna-1962-0713
11. P. Suppan, *Chemical Physics Letters,* **94(3)**,272(1983),https://doi.org/10.1016/0009-2614(83)87086-9
12. N.G. Bakhshiev, *Optics and Spectroscopy,* **16**, 821(1964)
13. J. Kabatc, B. Ośmiałowski and J. Pączkowski, *Spectrochimica Acta Part A: Molecular and Biomolecular Spectroscopy,* **63(3)**, 524(2006), https://doi.org/https://doi.org/10.1016/j.saa.2005.05.039
14. J. Basavaraja, S. Kumar, S.R. Inamdar and M.N. Wari, *Spectrochimica Acta Part A: Molecular and Biomolecular Spectroscopy,* **154**, 177(2016), https://doi.org/10.1016/j.saa.2015.10.020
15. W. Kohn and L. J. Sham, *Physical Review* **140(4A)**, A1133(1965), https://doi.org/10.1103/PhysRev.140.A1133
16. M.W. Wong, M.J. Frisch and K.B. Wiberg, *Journal of the American Chemical Society,* **113(13)**, 4776(1991), https://doi.org/10.1021/ja00013a010
17. E.M. Breitung, C.F. Shu and R.J. McMahon, *Journal of the American Chemical Society,* **122(6)**, 1154(2000), https://doi.org/10.1021/ja9930364

[RJC-9300/2025]